DOI: 10.1002/chem.200901471

The Effect of Backbone Stereochemistry on the Folding of Acyclic $\beta^{2,3}$-Aminoxy Peptides

Yu-Hui Zhang,[a, b] Kesheng Song,[a] Nian-Yong Zhu,[a] and Dan Yang*[a]

Abstract: As a new type of foldamer, β-aminoxy peptides have the ability to adopt novel β N−O turns or β N−O helices in solution. Herein, we describe a new subclass of β-aminoxy peptide, that is, peptides of acyclic $\beta^{2,3}$-aminoxy acids ($NH_2OCHR_1CHR_2COOH$), in which the presence of two chiral centers provides insight into the effect of backbone stereochemistry on the folding of β-aminoxy peptides. Acyclic $\beta^{2,3}$-aminoxy peptides with *syn* and *anti* configurations have been synthesized and their conformations investigated by NMR, IR, and circular dichroism (CD) spectroscopic, and X-ray crystallographic analysis. The β N−O turns or β N−O helices, which feature nine-membered rings with intramolecular hydrogen bonds and have been identified previously in peptides of β^3- and $\beta^{2,2}$-aminoxy acids, are also predominantly present in the acyclic $\beta^{2,3}$-aminoxy peptides with a *syn* configuration and N−O bonds *gauche* to the C_α−C_β bonds in both solution and the solid state. In the acyclic $\beta^{2,3}$-aminoxy peptides with an *anti* configuration, an extended strand (i.e., non-hydrogen-bonded state) is found in the solid state, and several conformations including non-hydrogen-bonded and intramolecular hydrogen-bonded states are present simultaneously in nonpolar solvents. These results suggest that the backbone stereochemistry does affect the folding of the acyclic $\beta^{2,3}$-aminoxy peptides. Theoretical calculations on the conformations of model acyclic $\beta^{2,3}$-aminoxy peptides with different backbone stereochemistry were also conducted to elucidate structural characteristics. Our present work may provide useful guidelines for the design and construction of new foldamers with predicable structures.

Keywords: aminoxy acids · conformation analysis · foldamers · peptidomimetics · stereochemistry

Introduction

In recent years, various unnatural oligomers with well-defined secondary structures (termed "foldamers") have been created and their conformational characteristics intensely studied[1] to reveal attractive architectures that could serve promising biological functions, such as cellular penetration, antibiotic activity, molecular recognition, and anion channels.[2] In an effort to develop novel peptidomimetic foldamers, we found that peptides made of aminoxy acids can adopt fascinating, rigid, yet predictable secondary structures. Up to this point, our studies primarily focused on two types of aminoxy peptide, α-aminoxy acids[3] and β-aminoxy acids[4] (Scheme 1). In comparison with natural amino acids, the N−O bond in aminoxy acids has unusual torsional characteristics that arise from repulsion between the lone pairs of electron on the N and O atoms. Thus, the backbone of aminoxy peptides is more rigid than that of natural peptides. For α-aminoxy peptides, 1.8_8 helices (i.e., α N−O helices that comprise α N−O turns; Scheme 1) were observed in peptides that contain as few as two residues and were independent of side chains.[3] α-Aminoxy peptides have been successfully used in the construction of anion receptors and channels.[5] Compared with α-aminoxy peptides, β-aminoxy peptides have extra β-carbon atoms in the backbone, thus leading to greater variations in substitution patterns (Scheme 2). Previous studies by our group indicated that β-aminoxy peptides can adopt novel β N−O turns or β N−O helices, which involve nine-membered rings with hydrogen

[a] Prof. Dr. Y.-H. Zhang, Dr. K. Song, Dr. N.-Y. Zhu, Prof. Dr. D. Yang
Department of Chemistry
The University of Hong Kong
Pokfulam Road, Hong Kong (China)
Fax: (+852) 2859-2159
E-mail: yangdan@hku.hk

[b] Prof. Dr. Y.-H. Zhang
Britton Chance Center for Biomedical Photonics
Wuhan National Laboratory for Optoelectronics
Huazhong University of Science and Technology
1037 Luoyu Road, Wuhan 430074 (China)

Supporting information for this article is available on the WWW under http://dx.doi.org/10.1002/chem.200901471.

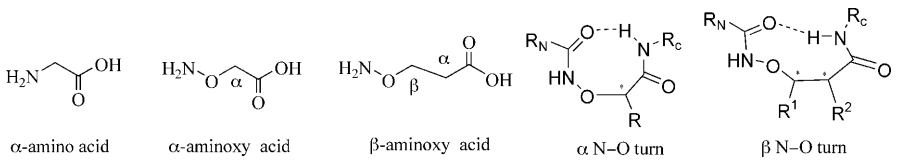

Scheme 1. α-Aminoxy acids[3] and β-aminoxy acids.[4]

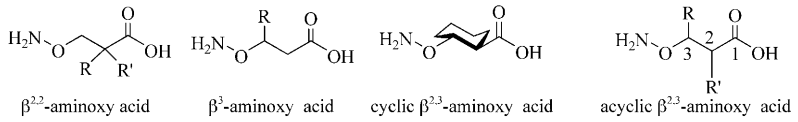

Scheme 2. β-Aminoxy peptides.

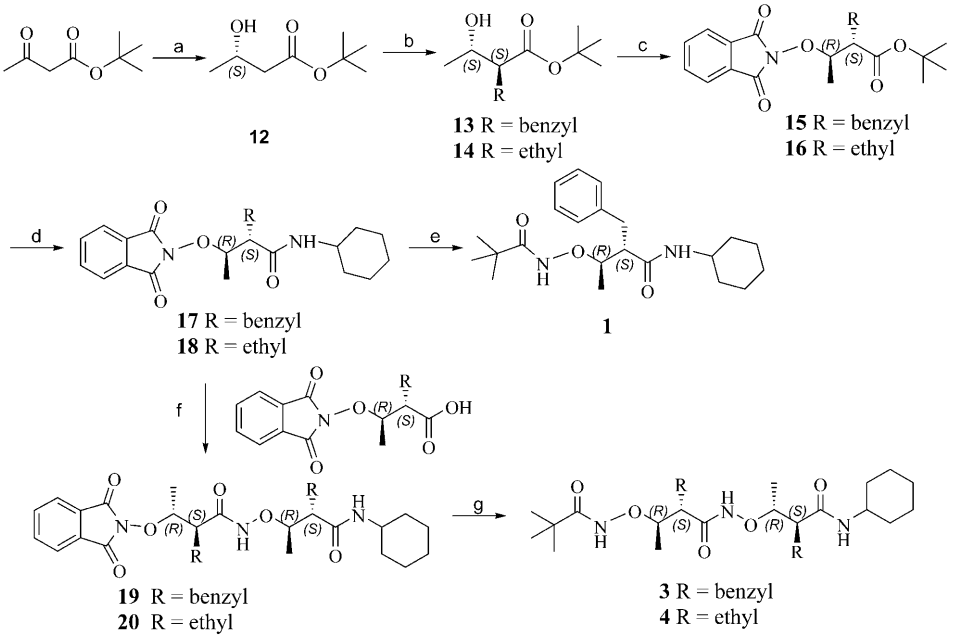

Scheme 3. Synthesis of **1**, **3**, and **4**. Reagents and conditions: a) Baker's yeast, petroleum ether/H_2O (63% yield, 93% *ee*); b) LDA, BnBr or CH_3CH_2I, THF, HMPA (60–70% yield); c) PhthN–OH, Ph_3P, DIAD, CH_2Cl_2 (58–64% yield); d) 1. TFA, CH_2Cl_2; 2. EDCI, HOBt, CH_2Cl_2, cyclohexylamine (65–71% overall yield); e) 1. $NH_2NH_2{\cdot}H_2O$, CH_3OH, CH_2Cl_2; 2. 10% $NaHCO_3$, $(CH_3)_3CHCOCl$, CH_3OH, CH_2Cl_2 (59% overall yield); f) 1. $NH_2NH_2{\cdot}H_2O$, CH_3OH, CH_2Cl_2; 2. EDCI, HOAt, CH_2Cl_2 (63–73% overall yield); g) 1. $NH_2NH_2{\cdot}H_2O$, CH_3OH, CH_2Cl_2; 2. 10% $NaHCO_3$, $(CH_3)_3CHCOCl$, CH_3OH, CH_2Cl_2 (61–68% overall yield). DIAD = diisopropyl azodicarboxylate, EDCI = 1-(3-dimethylaminopropyl)-3-ethylcarbodiimide hydrochloride, HMPA = hexamethylphosphoramide, LDA = lithium diisopropylamide, HOBt = 1-hydroxybenzotriazole, HOAt = 1-hydroxyazabenzotriazole, TFA = trifluoroacetic acid.

bonds between the neighboring residues, and that the local structures of the β N–O turns and β N–O helices vary slightly for different subclasses of β-aminoxy peptide (Scheme 2).[4] For example, the N–O bonds are *anti* to the C_α–C_β bonds in $\beta^{2,2}$-aminoxy peptides, whereas these bonds can be either *anti* or *gauche* in β^3-aminoxy peptides, depending on the size of the side chains (Scheme 2). Therefore, the extra β-carbon atoms in acyclic β-aminoxy peptides permit considerable conformational flexibility. For cyclic $\beta^{2,3}$-aminoxy peptides (Scheme 2), in which the α- and β-carbon atoms are part of an aliphatic ring (either a cyclopentane or cyclohexane unit), the N–O bonds are *anti* to the C_α–C_β bonds, independent of the ring size, thus indicating that the aliphatic rings increase the rigidness of the backbone.[6]

Another factor that is important in determining the folding of foldamers is the backbone stereochemistry; for example, $\beta^{2,3}$-peptides constructed with *trans*-2-aminocyclopentanecarboxylic acid (ACPC) favor a 12-helix structure,[7] whereas those constructed with *cis*-ACPC favor a strand structure.[8] Studies on acyclic disubstituted $\beta^{2,3}$-peptides have indicated that a 14-helix structure is present in α,β-*anti*-dialkyl $\beta^{2,3}$-peptides[9] (with the same configuration at the α- and β-carbon atoms), and sheet structures are favored in α,β-*syn*-dialkyl $\beta^{2,3}$-peptides (with different configurations at the α- and β-carbon atoms).[10] For $\gamma^{2,4}$-peptides with different configurations, reverse turns and helices are found.[11]

To investigate whether the backbone stereochemistry affects the secondary structures of β-aminoxy peptides, we prepared and characterized a novel subclass of β-aminoxy peptide, acyclic $\beta^{2,3}$-aminoxy peptides (4-oxa-γ-peptides). The presence of two chiral centers in the monomer unit (acyclic $\beta^{2,3}$-aminoxy acid; Scheme 2) allows us to examine the effect of backbone stereochemistry on the folding of β-aminoxy peptides. NMR, IR, and circular dichroism (CD) spectroscopic, and X-ray crystallographic analysis with computer simulation were used to elucidate the structural features of these acyclic $\beta^{2,3}$-aminoxy peptides. Our results lay the groundwork for predicting the conformation of β-aminoxy peptides and may help to guide efforts in constructing new foldamers with useful functions.

Results and Discussion

Synthesis of acyclic $\beta^{2,3}$-aminoxy peptides 1–7: Peptides **1–7** were synthesized as shown in Schemes 3–5 (see the Supporting Information for further details).

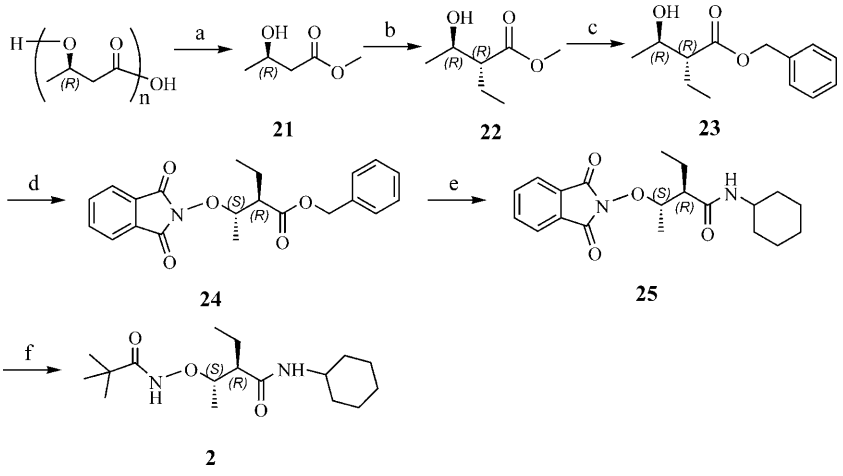

Scheme 4. Synthesis of **2**. Reagents and conditions: a) CH_3OH, H_2SO_4, $ClCH_2CH_2Cl$; b) LDA, CH_3CH_2I, THF, HMPA (52% yield); c) 1. LiOH, CH_3OH, H_2O; 2. 20% Cs_2CO_3, BnBr, DMF (88% overall yield); d) PhthN–OH, Ph_3P, DIAD, CH_2Cl_2 (35% yield); e) 1. Pd/C, H_2, CH_3OH, $CHCl_3$; 2. EDCI, HOBt, CH_2Cl_2, cyclohexylamine (65% overall yield); f) 1. $NH_2NH_2{\cdot}H_2O$, CH_3OH, CH_2Cl_2; 2. 10% $NaHCO_3$, $(CH_3)_3CHCOCl$, CH_3OH, CH_2Cl_2 (61% overall yield).

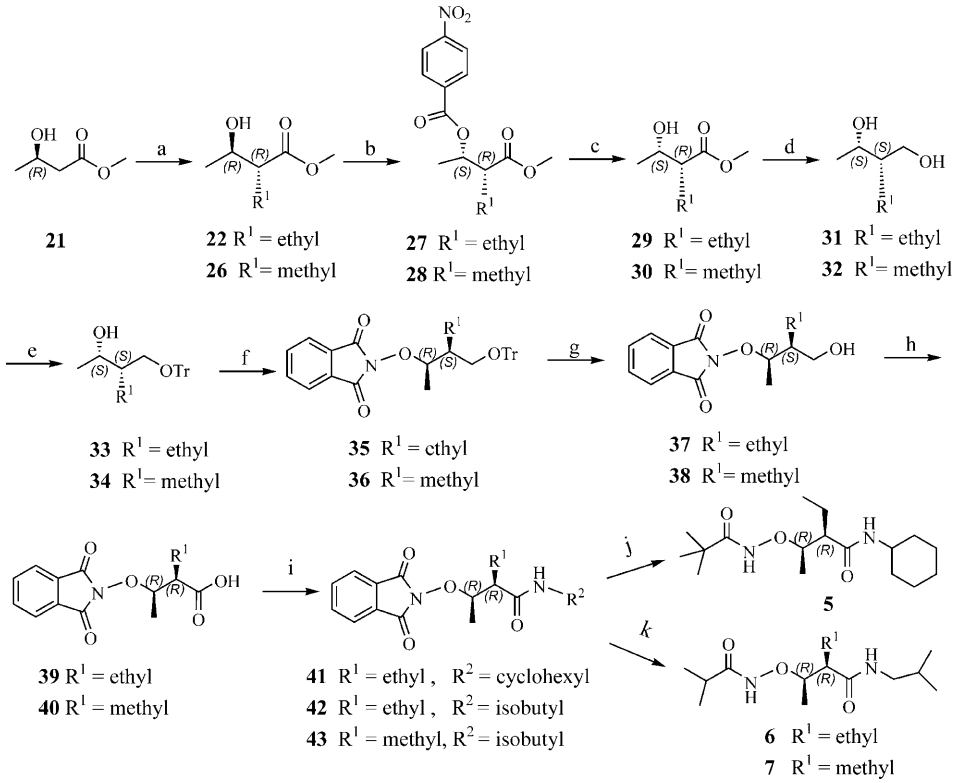

Scheme 5. Synthesis of **5–7**. Reagents and conditions: a) LDA, CH_3CH_2I or CH_3I, THF, HMPA (43–52% yield); b) 4-$NO_2C_6H_4COOH$, Ph_3P, DEAD, THF (50–71% yield); c) NaN_3, CH_3OH, 45°C (45–65% yield); d) $LiAlH_4$, Et_2O; e) TrCl, DMAP, DMF, Et_3N (73–95% overall yield); f) PhthN–OH, PPh_3, DIAD, CH_2Cl_2 (80–85% yield); g) HCOOH, CH_2Cl_2 (60–73% yield); h) $NaIO_4$, $RuO_2{\cdot}H_2O$, $CH_3CN/CCl_4/H_2O$/acetone 1:1:1.4:0.3; 1. EDCI, HOAt, CH_2Cl_2, cyclohexylamine or isobutylamine (55–78% overall yield); j) 1. $NH_2NH_2{\cdot}H_2O$, CH_3OH, CH_2Cl_2; 2. 10% $NaHCO_3$, $(CH_3)_3CHCOCl$, CH_3OH, CH_2Cl_2 (65% overall yield); k) 1. $NH_2NH_2{\cdot}H_2O$, CH_3OH, CH_2Cl_2; 2. EDCI, HOAt, CH_2Cl_2, $(CH_3)_2CHCOOH$ (56–60% overall yield). DEAD = diethyl azodicarboxylate, DMAP = 4-dimethylaminopyridine, TrCl = triphenymethyl chloride.

Conformational studies of compounds 1–7 by ^{1}H NMR spectroscopy: Two ^{1}H NMR spectroscopic methods based on 1) the concentration dependence of the chemical shifts of the amide protons[12] and 2) the gradual addition of a strong hydrogen-bond acceptor, such as deuterated dimethyl sulfoxide ($[D_6]$DMSO), to a dilute solution of the peptide in a non-hydrogen-bonding solvent, such as $CDCl_3$,[13] are commonly used to probe the formation of intramolecular hydrogen bonds by amide protons in linear peptides in solution. We applied these two methods to the characterization of the intramolecular hydrogen bonds present in the peptides of acyclic $\beta^{2,3}$-aminoxy acids.

Table 1 summarizes the chemical shifts of the amide protons in the ^{1}H NMR spectra of **1–7** at room temperature, among which **1–4** have a *syn* configuration and **5–7** have an *anti* configuration (Scheme 6). The protons of the *N*-oxy amide unit NH_b of **3** and **4** and the regular amide unit NH_c of **1–4** appeared unusually downfield and showed little change when the solutions were diluted from 50 to 1.56 mM in $CDCl_3$ ($\Delta\delta = 0.05$–0.16 ppm) or when $[D_6]$DMSO was added gradually to a 5 mM solution of **1–4** in $CDCl_3$ ($\Delta\delta = 0.07$–0.30 ppm; Table 1). In contrast, the signals of the *N*-oxy amide unit NH_a of **1–4** were found rather upfield and changed dramatically upon dilution in $CDCl_3$ ($\Delta\delta = 0.17$–0.74 ppm) or upon addition of $[D_6]$DMSO ($\Delta\delta = 1.70$–2.22 ppm; Table 1). These results suggest that the amide protons NH_b of **3** and **4** and NH_c of **1–4** form intramolecular hydrogen bonds, whereas the amide protons NH_a of **1–4** are accessible to the solvent.

For compounds **5–7** with an *anti* configuration, the signals from the amide protons NH_a were located at about $\delta =$ 8.6 ppm and were shifted substantially in the dilution studies and $[D_6]$DMSO addition studies. This outcome reveals that

Table 1. Chemical shifts (δ) and changes in the chemical shift ($\Delta\delta_{NH}$) of the amide protons of **1–7** in ^{1}H NMR spectroscopic dilution (dilu.) and in [D_6]DMSO addition studies (DMSO).

Comp.	NH_a [ppm]			NH_b [ppm]			NH_c [ppm]		
	δ[a]	$\Delta\delta$[b] (dilu.)	$\Delta\delta$[c] (DMSO)	δ[a]	$\Delta\delta$[b] (dilu.)	$\Delta\delta$[c] (DMSO)	δ[a]	$\Delta\delta$[b] (dilu.)	$\Delta\delta$[c] (DMSO)
1	8.21	0.17	1.82				8.00	0.054	0.33
2	8.35	0.24	1.70				7.76	0.097	0.42
3	8.24	0.45	2.22	11.42	0.093	0.30	7.79	0.070	0.068
4	8.43	0.74	2.08	11.48	0.16	0.26	7.89	0.14	0.098
5	8.67	0.15	1.20				6.31	0.13	1.05
6	8.59	0.51	1.81				6.83	0.25	1.06
7	8.34		1.91				7.07		0.96

[a] δ = Chemical shift of the amide NH protons obtained from the ^{1}H NMR spectrum of the indicated compound (5 mM, CD_2Cl_2, room temperature; there was little change in the chemical shift of the amide protons of **1–7** below 5 mM). [b] Dilution study: solutions of **1–7** in $CDCl_3$ were diluted from 50 to 1.56 mM at room temperature ($\Delta\delta_{Dilution} = \delta_{50\,mM} - \delta_{1.56\,mM}$). [c] [$D_6$]DMSO addition study: [$D_6$]DMSO (50 μL) was added gradually to a solution of **1–7** (5 mM) in $CDCl_3$ (0.5 mL) at room temperature ($\Delta\delta_{DMSO} = \delta_{50\,\mu L\ of\ DMSO} - \delta_{0\,\mu L\ of\ DMSO}$).

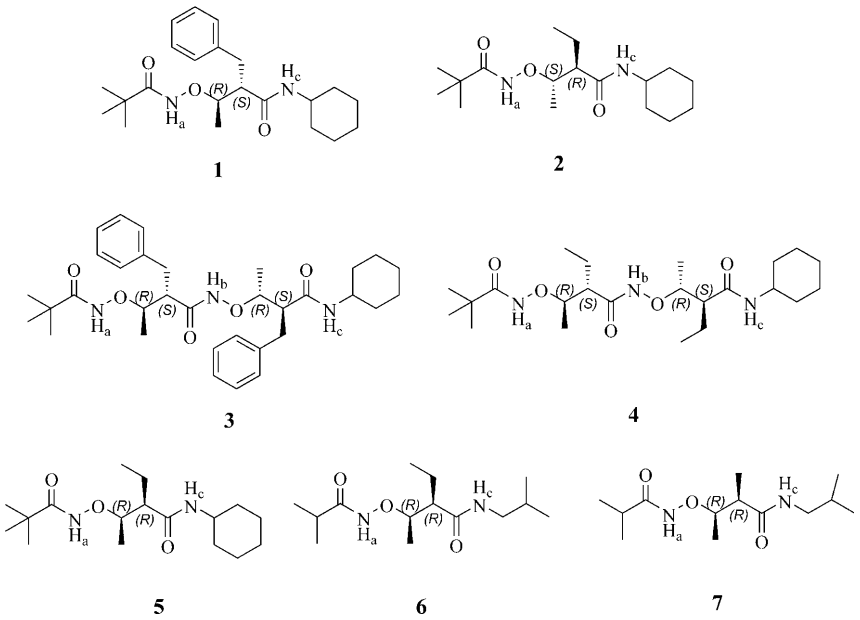

Scheme 6. Compounds **1–7** with *syn* or *anti* configurations.

the protons of the *N*-oxy amide unit NH_a are solvent exposed, similar to the NH_a protons in **1–4**. Compared with the NH_c protons in **1–4**, the NH_c protons in **5–7** appeared relatively upfield (δ = 6.31–7.07 ppm), thus suggesting that non-hydrogen-bonded states exist partially in each case (Table 1). This conclusion is further supported by the evidence that a relatively large $\Delta\delta$ shift for the amide protons NH_c in **5–7** was observed in the dilution studies and [D_6]DMSO addition studies (Table 1). When the protecting groups of the C or N terminus were changed from large to small groups (as in **5** and **6**, respectively) or when the substituent at C_α was changed from an ethyl to a methyl group (as in **6** and **7**, respectively), the amide proton NH_c shifted downfield gradually, thus implying a slight increase in the populations of the hydrogen-bonded states.

Conformational studies of compounds 1–7 by IR spectroscopy: The observed value of each amide proton in the ^{1}H NMR spectra usually represents a population-weighted average of non-hydrogen-bonded and hydrogen-bonded states to account for the rapid exchange between these states. In contrast, the timescale of IR spectroscopic measurements is short enough to clearly distinguish the N–H stretching signals of the hydrogen-bonded and non-hydrogen-bonded states. Therefore, the data from the N–H stretching region of the IR spectra provide insight into the degree of hydrogen-bond existence in nonpolar solvents.[3,4]

Previous studies have shown that the IR absorption peaks of the non-hydrogen-bonded amide NH appear between $\tilde{\nu}$ = 3400 and 3450 cm^{-1} and the peaks of the non-hydrogen-bonded *N*-oxy amide NH are between $\tilde{\nu}$ = 3340 and 3400 cm^{-1}. The absorption peaks that correspond to the hydrogen-bonded normal amide and *N*-oxy amide appear around $\tilde{\nu}$ = 3300 and 3200 cm^{-1}, respectively.[3,4]

Figure 1 presents the N–H stretching region of the FTIR spectra of **1–7**. The spectra were recorded at a very low concentration (2 mM), such that intermolecular hydrogen bonding is unlikely to occur (Table 1). We observed three major peaks for **1** and **2** and four major peaks for **3** and **4** (Figure 1): the absorptions peaks in the region $\tilde{\nu}$ = 3399–3405 cm^{-1} correspond to the non-hydrogen-bonded *N*-oxyamide NH_a groups at the N termini; the large peaks in the region $\tilde{\nu}$ = 3281–3295 cm^{-1} are due to the stretching of the hydrogen-bonded C-terminal amide NH_c groups; the small shoulder peaks at $\tilde{\nu}$ = 3430–3432 cm^{-1} are assigned to the N–H stretching bands of the non-hydrogen-bonded amide NH_c groups at the C termini; and the fourth peak in the IR spectra of **3** and **4** at $\tilde{\nu}$ = 3201 cm^{-1} comes from the stretching of intramolecular hydrogen-bonded NH_b unit. The small peaks at $\tilde{\nu}$ = 3430–3432 cm^{-1} indicate that negligible populations of the non-hydrogen-bonded conformation of **1–4** are present in CH_2Cl_2. For **5–7**, the peaks in the regions $\tilde{\nu}$ = 3395–3399 and 3308–3326 cm^{-1} are assigned to the stretching of the non-hydrogen-bonded NH_a and weakly hydrogen-bonded NH_c units, respectively (Figure 1), and the large peaks at $\tilde{\nu}$ = 3430–

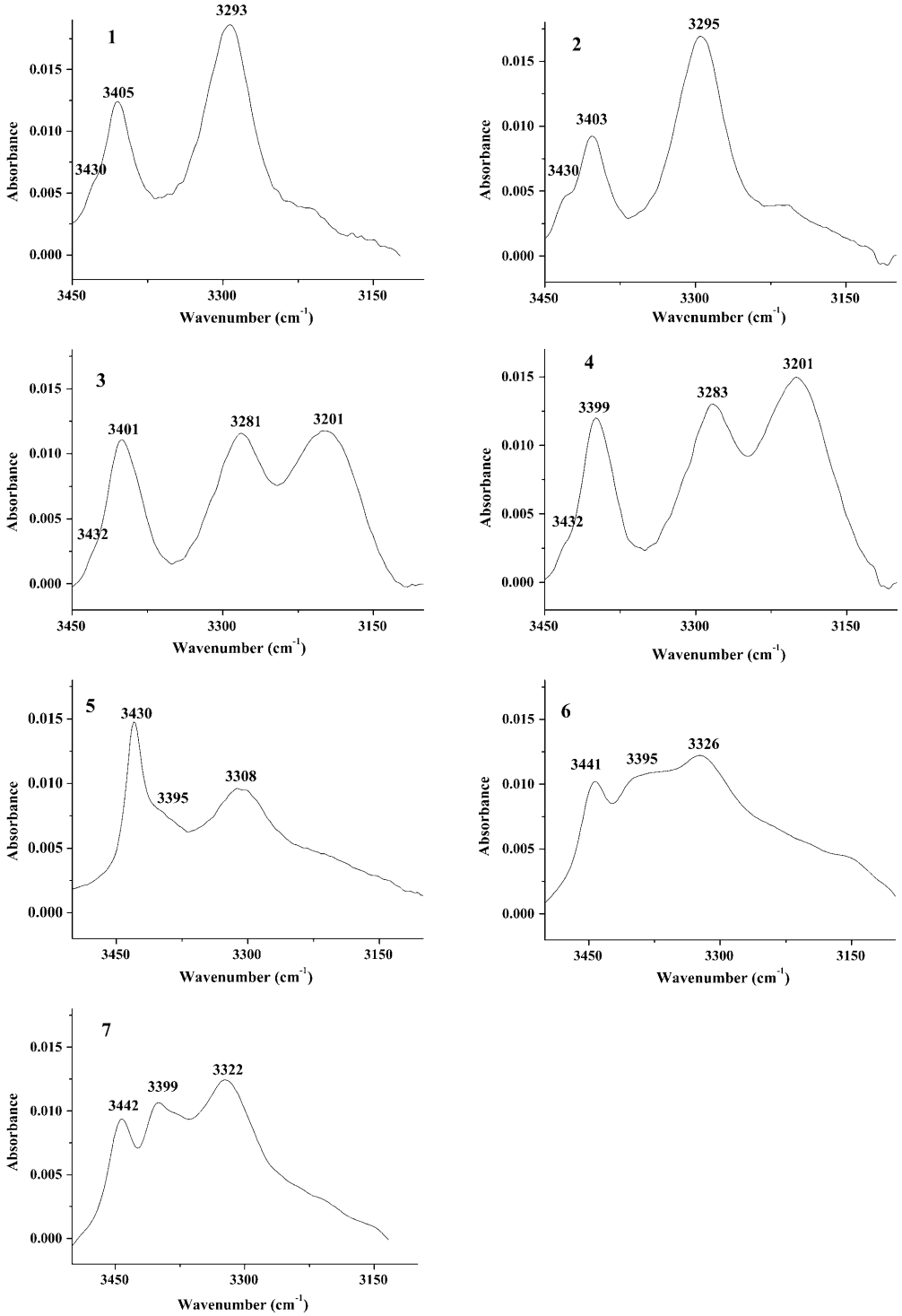

Figure 1. The N–H stretching region of the FTIR spectra of **1–7** (2 mM, CH_2Cl_2, at room temperature) after subtraction of the spectrum of pure CH_2Cl_2.

3442 cm^{-1} suggest a substantial population of non-hydrogen-bonded NH_c units, especially in **5**. These results are in good agreement with the observations from the ^1H NMR spectroscopic studies.

X-ray crystallographic analysis of 1 and 5: From our ^1H NMR and IR spectroscopic studies, information about whether intramolecular hydrogen bonds are formed and to what extent hydrogen-bond existence is achieved was obtained, but the structural features of these intramolecular hydrogen bonds, such as ring size and dihedral angles of the bonds, are still unknown. To clarify the characteristics of the secondary structures formed in acyclic $\beta^{2,3}$-aminoxy peptides, we attempted to grow crystals. Fortunately, suitable

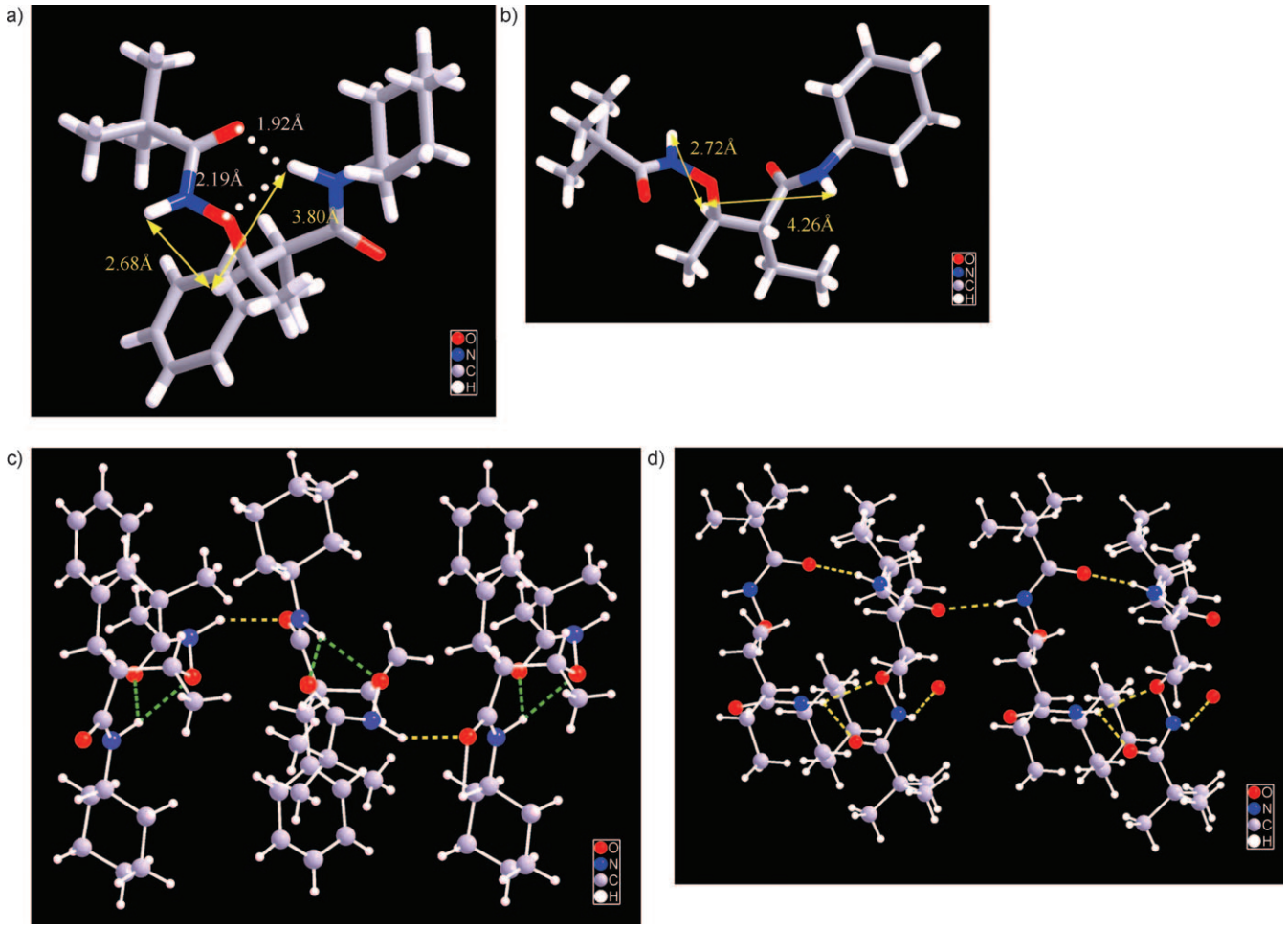

Figure 2. The solid-state structures of a) **1** and b) **5**. The solid-state packing patterns of c) **1** containing three molecules and d) **5** containing four molecules. Dotted lines in yellow indicate intermolecular hydrogen bonds and dotted lines in green indicate intramolecular hydrogen bonds.

crystals of **1** and **5** for single-crystal X-ray structural analysis were obtained from CH_2Cl_2/*n*-hexane. The X-ray crystallographic structure shown in Figure 2a reveals that **1** adopts a β N–O turn structure, thus bearing high similarity to that formed in compound **8** of β^3-aminoxy acid, which involves a nine-membered ring with hydrogen bonds between the C=O_i and NH_{i+2}, and is stabilized further by another six-membered ring with hydrogen bonds between the NH_{i+2} and NO_{i+1} units.[4b] The N–O bond in **1** is *gauche* to the C_α–C_β bond with a dihedral angle $\measuredangle NOC_\beta C_\alpha$ of 77.95° (Table 2). The molecules of **1** pack in an antiparallel fashion with an intermolecular hydrogen bond between two adjacent molecules (Figure 2c).

For compound **5**, there are two molecules present in each asymmetric unit of the crystal but with slightly different conformations (Table 2). No intramolecular hydrogen bonds are observed in the crystal structures (Figure 2b). Three intermolecular hydrogen bonds are observed between these two molecules in the same unit, and one unit is connected to an adjacent unit by the fourth intermolecular hydrogen bond. A water molecule also forms a hydrogen bond with an amide proton in each unit (Figure 2d). All the molecules

Table 2. Torsional angles[a] of **1** and **5** of $\beta^{2,3}$-aminoxy acids and model **8**[4b] of β^3-aminoxy acids in their solid-state structures.

Compound		ϕ [°]	θ [°]	ϕ [°]	ψ [°]
1		−113.50	77.95	73.30	−70.47
8[a]		−115.85	70.42	77.49	−70.10
5	conformation A	123.84	178.48	−44.39	−112.07
	conformation B	108.69	160.67	−66.30	135.26

[a]

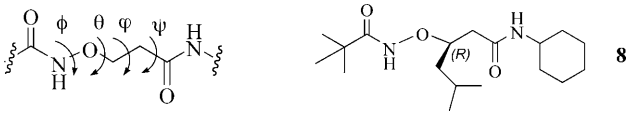

8

adopt "extended" strand conformations with the N–O bond *anti* to the C_α–C_β bond (dihedral angle $\measuredangle NOC_\beta C_\alpha$: 178.48 or 160.67°). These findings are in contrast with the results of the ^{1}H NMR and IR spectroscopic studies, which indicated that both intramolecular hydrogen-bonded or non-hydrogen-bonded conformations of **5** exist simultaneously in solution, possibly because the "extended" strand is more favorable in the solid state in which the molecules are packed at an exceedingly "high concentration". A disagreement be-

tween the structures in solution and in the solid state was also noted in the β^3-aminoxy peptides, in which the sheet structures (with intermolecular hydrogen bonds) and β N−O turns (with intramolecular hydrogen bonds) are formed in the solid state and in solution, respectively.[4b]

2D NOESY studies of 1–7: The 2D NOESY spectroscopic method was used to investigate the secondary structures of **1–7** in solution (Figure 3). Similar NOE patterns were obtained for **1** and **2**: stronger NOE interactions between the NH_a and CH_β protons and weaker NOE interactions between the NH_c and CH_β protons. This observation agrees well with the evidence that the H···H distance between the NH_a and CH_β units in the solid-state structure of **1** is approximately 2.68 Å, which is shorter than the distance between the NH_c and CH_β units (ca. 3.80 Å; Figure 2a). The similarity of the NOE patterns observed for **1** and **2** also suggest that the difference in the side chain at the C_α position has a limited effect on the secondary structures of **1** and **2**. It is most likely that both **1** and **2** preferentially adopt a β N−O turn conformation with the N−O bond *gauche* to the C_α–C_β bond in solution and the solid state. The NOE patterns observed for **3** and **4** are analogous to those for **1** and **2**; therefore, the β N−O helices with two consecutive β N−O turns are the dominant conformations of **3** and **4** in solution.

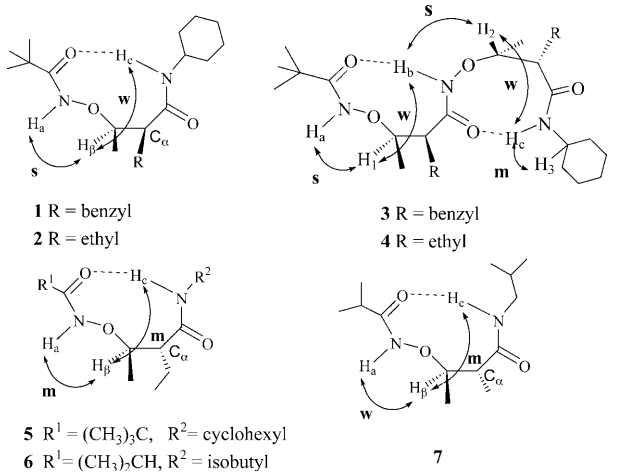

Figure 3. Summary of the NOE interactions observed (s = stronger, m = medium, w = weaker NOE interactions) in the NOESY spectra of **1–7** (5 mM, CD_2Cl_2, room temperature).

The NOE interactions obtained for **5** reveal a distinct pattern: a medium NOE interaction between the NH_a and CH_β protons and a medium NOE interaction between the NH_c and CH_β protons (Figure 3). The NOE pattern does not agree with the crystal structure of **5**, in which the H···H distance between the NH_a and CH_β protons (ca. 2.72 Å) is much shorter than the distance between the NH_c and CH_β protons (ca. 64.26 Å; Figure 2b). This result also suggests that the conformation of **5** in solution is a little different to the conformation in the solid state. The NOE pattern for **6** with a small protecting group at the N terminus is similar to the pattern for **5**. However, there is a different NOE pattern for **7**, which has a smaller substituent (methyl group) at the C_α position than **5** and **6** (which have an ethyl group at this position), compared to **5** and **6**, that is, a weak NOE interaction between the NH_a and CH_β protons and a medium NOE interaction between the NH_c and CH_β protons (Figure 3). This difference suggests that the substituent at the C_α position slightly affects the conformations of $\beta^{2,3}$-aminoxy peptides with an *anti* configuration.

CD studies of 2 and 4–7: CD spectroscopy has been successfully employed on an extensive scale to characterize the secondary structures of foldamers.[3,4,14] We used CD spectroscopy as an additional tool to determine the conformation of the homochiral peptides of acyclic $\beta^{2,3}$-aminoxy acids. The CD spectra of **2** and **4–7** in CF_3CH_2OH are shown in Figure 4; however, CD spectra of **1** and **3** in CF_3CH_2OH could not be obtained due to poor solubility. The CD curves of **2** and **4** in CF_3CH_2OH, which constitute nearly mirror images of each other for their opposite chirality, are very similar to those of β^3-aminoxy peptides[4b] with a maximum absorption at approximately $\lambda = 202$ nm (Figure 4A), thus suggesting that the β N−O turn and β N−O helix are adopted predominantly in **2** and **4**, respectively. The CD absorption peaks of **5** and **7** determined at different concentrations showed negligible changes, thus implying that there was no aggregation (Figure 4B). The CD curves observed for **5–7** (Figure 4B) are similar to each other with a maximum absorption at approximately $\lambda = 198$ nm and zero crossing at

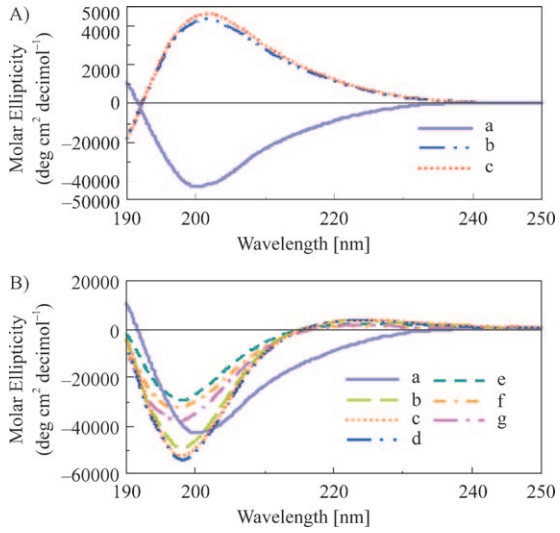

Figure 4. A) CD spectra of **2** and **4** (CF_3CH_2OH, room temperature): a) **2** at 0.5 mM, b) **4** at 0.5 mM, and c) **4** at 5 mM. B) CD spectra of **2** and **5–7** (CF_3CH_2OH, room temperature): a) **2** at 0.5 mM, b) **5** at 0.5 mM, c) **5** at 5 mM, d) **5** at 10 mM, e) **6** at 0.2 mM, f) **7** at 0.5 mM, and g) **7** at 5 mM. The spectra have been normalized for the concentration of the compound and the number of backbone amide residues.

approximately $\lambda = 217$ nm, but differ slightly from the curves of **2** and **4**, thus suggesting that the secondary structures in **5**–**7** are, to some extent, different from the structures in **2** and **4**.

Theoretical calculations: We carried out theoretical calculations to elucidate the conformational features of acyclic $\beta^{2,3}$-aminoxy peptides with different backbone stereochemistry and different substituents at the C_α positions. All the calculations were conducted with the Gaussian98 program.[15] The geometry of each structure was fully optimized by the B3LYP/6-311G** method,[16] and vibration-frequency calculations were subsequently performed. The energies were evaluated by the MP2/6-311G** method[17] based on B3LYP/6-311G** geometries. Solvent effects were estimated from the SCIPCM model[18] by the B3LYP/6-311G** method. The final relative energies of the different conformations were estimated by using Equation (1) , which has been shown to be highly robust for other peptide systems.[4a,19]

$$\Delta G = \Delta E(\mathrm{MP2}) + [\Delta E(\mathrm{B3LYP,\ solvent}) - \Delta E(\mathrm{B3LYP,\ gas})] + \text{enthalpy correction} - T\Delta S \quad (1)$$

Model structures **8** and **9** (Scheme 7) are the simulations of **1** and **2** (Scheme 6), respectively, which have the same configuration (*syn*), but a different substituent at the C_α position. Figure 5 displays the five stable conformations of model **8**. In consideration of relative energies, structure **8a**, which features strong, nine-membered-ring intramolecular hydrogen bonding, is the most stable conformation. Compound **8b** is distinguished from **8a** by its dihedral angles θ of approximately 79.2° in **8a** (*gauche*) and −161.4° in **8b** (*anti*) (Scheme 7). Thus, **8b** is less stable than **8a** due to a geometrical distortion. Structures **8c** and **8d** also possess nine-membered-ring intramolecular hydrogen bonding, though they are much less stable as a result of weaker hydrogen bonding and geometrical distortions. Structure **8e** has seven-membered-ring intramolecular hydrogen bonding and is less stable in CH_2Cl_2 than **8a** by approximately 2.5 kcal mol^{-1}. The calculations, therefore, suggest that the dominant conformation of model **8** in CH_2Cl_2 is **8a**, which features nine-membered-ring intramolecular hydrogen bonding and a *gauche* dihedral angle θ. The H···H distances NH_a···C_βH and NH_b···C_βH in **8a** are approximately 2.71 and 4.03 Å, respectively, which are in good agreement with the solid-state structure (Figure 2a) and the strong/weak NOE pattern observed for **1** (Figure 3).

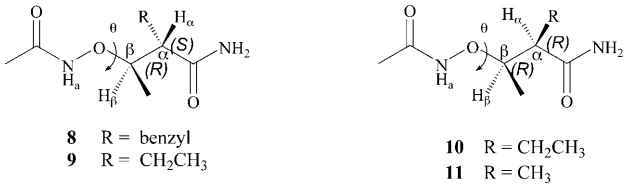

Scheme 7. Models **8**–**11**.

Figure 6 shows the five stable conformations of model **9**. The nine-membered-ring intramolecular hydrogen-bonded conformation **9a**, which is similar to **8a**, is the most stable and in agreement with the strong/weak NOE pattern observed for **2** in the 2D NOESY spectrum (Figure 3). The results suggest that changing the substituent at C_α from a benzyl group to an ethyl group does not affect the secondary structures of $\beta^{2,3}$-aminoxy peptides with *syn* configurations.

The structural features of compounds **5**–**7** with *anti* configurations were calculated for models **10** and **11** (Scheme 7), respectively. Compared with **10**, **11** has a smaller substituent (methyl group) at C_α. The differences between the free energies of the calculated conformations for **10** and **11** (Figure 7 and 8, respectively) are much less than those energies for models **8** and **9** (Figure 5 and 6, respectively), thus suggest-

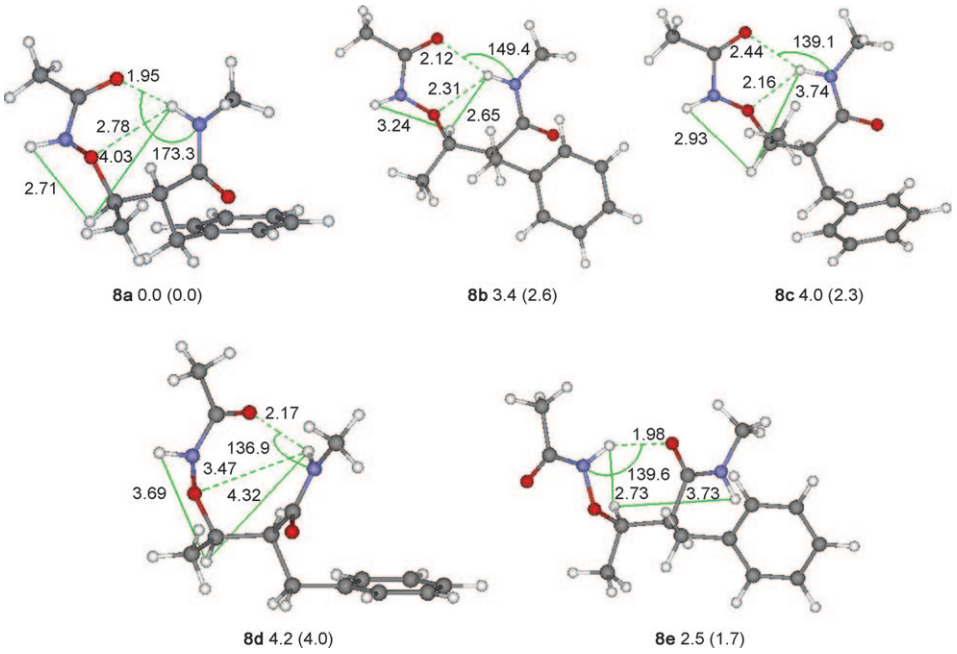

Figure 5. Calculated conformations of model **8**. The relative free energies (kcal mol^{-1}) were calculated at the MP2/6-311G** level in the gas phase and in CH_2Cl_2 (given in parentheses). The H···H distances of the NH_a···C_βH and NH_b···C_βH interactions, the hydrogen-bond lengths, and the angles of the NH_b···O interactions (Å) are indicated.

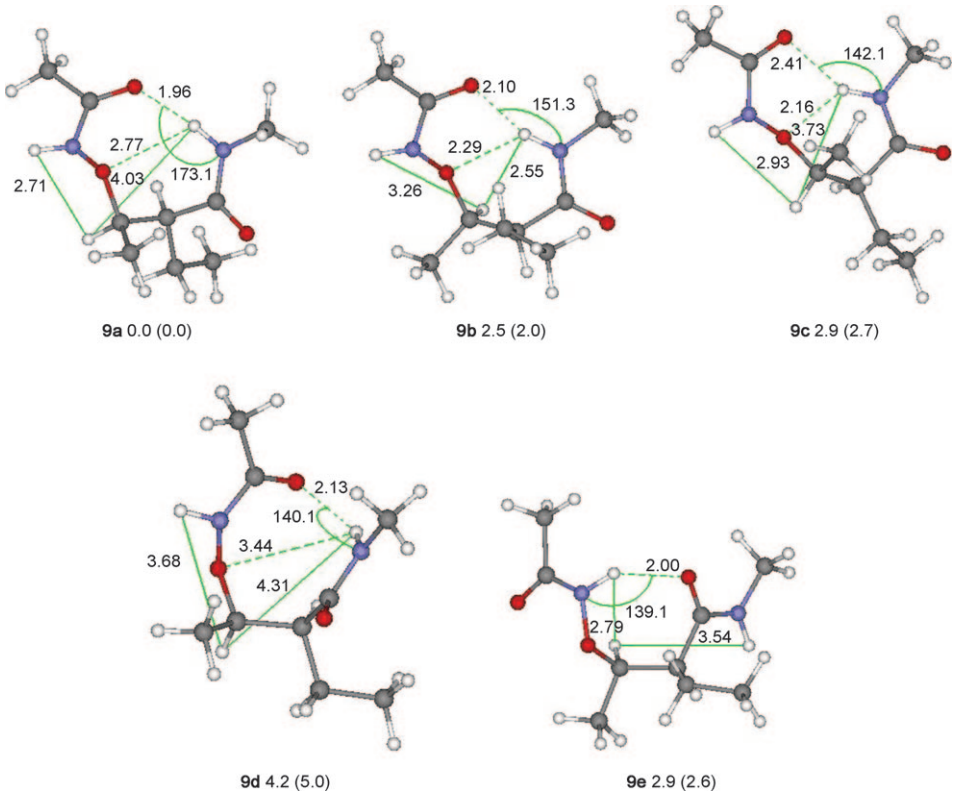

Figure 6. Calculated conformations of model **9**. The relative free energies (kcal mol^{-1}) were calculated at the MP2/6-311G** level in the gas phase and in CH_2Cl_2 (given in parentheses). The H···H distances of the NH_a···$C_\beta H$ and NH_b···$C_\beta H$ interactions, the hydrogen-bond lengths, and angles of the NH_b···O interactions (Å) are indicated.

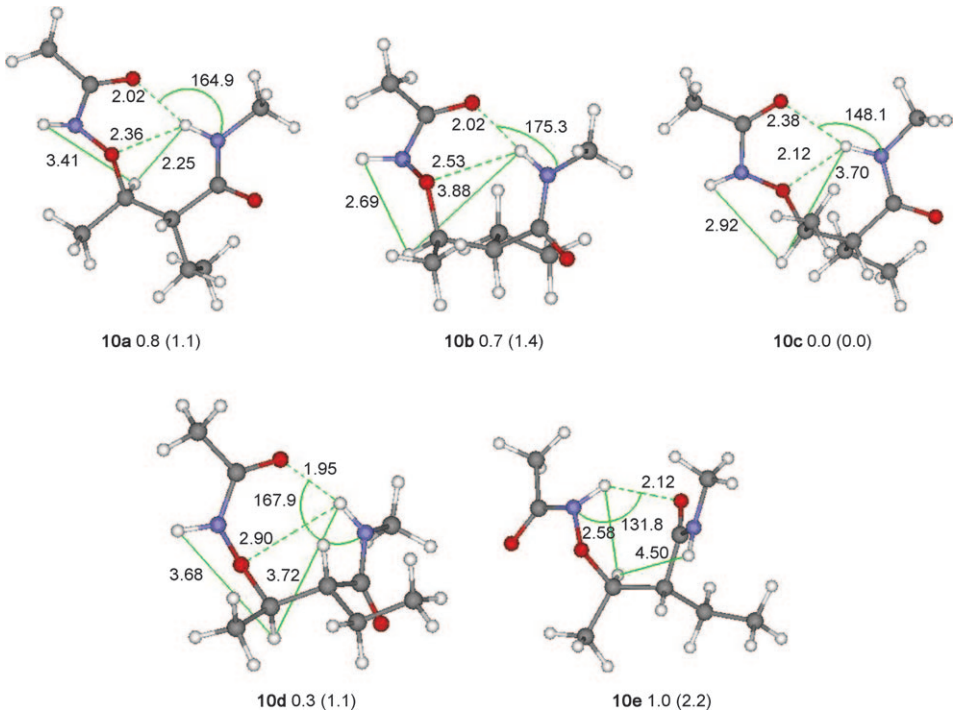

Figure 7. Calculated conformations of **10**. The relative free energies (kcal mol^{-1}) were calculated at the MP2/6-311G** level in the gas phase and in CH_2Cl_2 (given in parentheses). The H···H distances of the NH_a···$C_\beta H$ and NH_b···$C_\beta H$ interactions, the hydrogen-bond lengths, and angles of the NH_b···O interactions (Å) are indicated.

ing that **10** and **11** are much more flexible in their conformations. Thus, unlike **8**, which favors a single dominant conformation (i.e., **8a**), **10** and **11** possibly have a tendency to exist simultaneously in several variant conformations in solution. This interpretation was supported by the evidence that the weak/medium NOE pattern observed for **7** does not agree with any of the calculated conformations for **11** alone. Taken together, for **5**–**7**, several conformations may coexist in solution, whereas the percentages of these conformations may vary for each of these compounds, thus resulting in the different NOE patterns observed for **5**, **6** (medium/medium NOE pattern), and **7** (weak/medium NOE pattern). This outcome may explain why the CD spectra of **5**–**7** are different from those spectra of **2** and **4**, in which only one dominant conformation is favored.

Conclusions

In summary, we have synthesized and investigated the conformational preferences of acyclic $\beta^{2,3}$-aminoxy peptides with different backbone stereochemistry. For acyclic $\beta^{2,3}$-aminoxy peptides with *syn* configurations, the results from ^{1}H NMR, 2D NOESY, IR, and CD spectroscopic, and X-ray crystallographic studies agree well with each other and show consistency with theoretical calculations. In addition, the β N–O turns or β N–O helices, which have previously been found in the peptides of β^3- and $\beta^{2,2}$-aminoxy acids featuring nine-membered-ring intramolecular hydrogen bonding, are present predominantly in these acyclic $\beta^{2,3}$-aminoxy peptides with *syn* configurations. However, the local structures of the β N–O turns

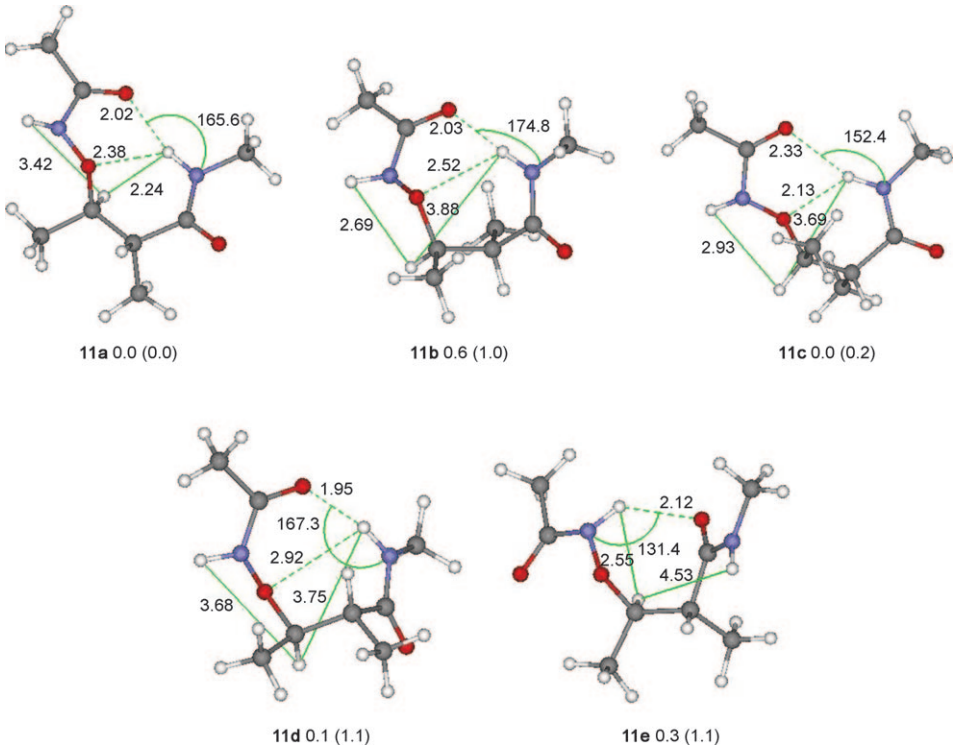

Figure 8. Calculated conformations of **11**. The relative free energies (kcal mol^{-1}) were calculated at the MP2/6-311G** level in the gas phase and in CH_2Cl_2 (given in parentheses). The H···H distances of the NH_a···$C_\beta H$ and NH_b···$C_\beta H$ interactions, the hydrogen-bond lengths, and angles of the NH_b···O interactions (Å) are indicated.

or β N–O helices in different subclasses of β-aminoxy peptide are different from each other. More specifically, the N–O bonds are *gauche* to the C_α–C_β bonds in acyclic $\beta^{2,3}$-aminoxy peptides with *syn* configurations, *anti* in $\beta^{2,2}$-aminoxy peptides, and either *anti* or *gauche* in β^3-aminoxy peptides depending on the size of the side chains.

The change of backbone stereochemistry from a *syn* to an *anti* configuration gives rise to the more complex conformations seen in acyclic $\beta^{2,3}$-aminoxy peptides with *anti* configurations. Theoretical calculations reveal that the differences between the free energies of the calculated conformations of models **10** and **11** are not large. This finding means that acyclic $\beta^{2,3}$-aminoxy peptides with *anti* configurations are much more flexible in their conformations and may explain why both intramolecular hydrogen-bonded states and non-hydrogen-bonded states are simultaneously observed in the ^{1}H NMR and IR spectra of compounds **5**–**7**. Only an extended strand with intermolecular hydrogen bonds was found in the solid state of **5**, which disagrees with the NOE pattern observed for **5** in solution. This disagreement may be accounted for by the crystal packing. Therefore, unlike acyclic $\beta^{2,3}$-aminoxy peptides with *syn* configurations, which favor only one dominant conformation both in solution and the solid state, acyclic $\beta^{2,3}$-aminoxy peptides with *anti* configurations seem to form several conformations simultaneously. The results presented herein may provide useful guidelines for the design of new foldamers.[20]

Acknowledgements

This study was supported by The University of Hong Kong and the Research Grants Council of Hong Kong (HKU 06/2C and HKU 7654/06M).

[1] a) S. H. Gellman, *Acc. Chem. Res.* **1998**, *31*, 173–180; b) J. Venkatraman, S. C. Shankaramma, P. Balaram, *Chem. Rev.* **2001**, *101*, 3131–3152; c) R. P. Cheng, S. H. Gellman, W. F. DeGrado, *Chem. Rev.* **2001**, *101*, 3219–3232; d) D. J. Hill, M. J. Mio, R. B. Prince, T. S. Hughes, J. S. Moore, *Chem. Rev.* **2001**, *101*, 3893–4011; e) D. Seebach, A. K. Beck, D. J. Bierbaum, *Chem. Biodiversity* **2004**, *1*, 1111–1239; f) D. Seebach, J. Gardiner, *Acc. Chem. Res.* **2008**, *41*, 1366–1375; g) W. S. Horne, S. H. Gellman, *Acc. Chem. Res.* **2008**, *41*, 1399–1408.

[2] a) C. M. Goodman, S. Choi, S. Shandler, W. F. DeGrado, *Nat. Chem. Biol.* **2007**, *3*, 252–262; b) X. Li, Y.-H. Wu, D. Yang, *Acc. Chem. Res.* **2008**, *41*, 1428–1438; c) A. D. Bautista, C. J. Craig, E. A. Harker, A. Schepartz, *Curr. Opin. Chem. Biol.* **2007**, *11*, 685–692.

[3] a) D. Yang, F.-F. Ng, Z.-J. Li, Y.-D. Wu, K. W. K. Chan, D.-P. Wang, *J. Am. Chem. Soc.* **1996**, *118*, 9794–9795; b) Y.-D. Wu, D.-P. Wang, K. W. K. Chan, D. Yang, *J. Am. Chem. Soc.* **1999**, *121*, 11189–11196; c) D. Yang, J. Qu, B. Li, F.-F. Ng, X.-C. Wang, K.-K. Cheung, D.-P. Wang, Y.-D. Wu, *J. Am. Chem. Soc.* **1999**, *121*, 589–590; d) D. Yang, B. Li, F.-F. Ng, Y.-L. Yan, J. Qu, Y.-D. Wu, *J. Org. Chem.* **2001**, *66*, 7303–7312; e) D. Yang, J. Qu, W. Li, D.-P. Wang, Y. Ren, Y.-D. Wu, *J. Am. Chem. Soc.* **2003**, *125*, 14452–14457; f) D. Yang, W. Li, J. Qu, S. W. Luo, Y.-D. Wu, *J. Am. Chem. Soc.* **2003**, *125*, 13018–13019; g) X. Li, D. Yang, *Chem. Commun.* **2006**, 3367–3379.

[4] a) D. Yang, Y.-H. Zhang, N.-Y. Zhu, *J. Am. Chem. Soc.* **2002**, *124*, 9966–9967; b) D. Yang, Y.-H. Zhang, B. Li, D.-W. Zhang, C.-Y. J. Chan, N.-Y. Zhu, S.-W. Luo, Y.-D. Wu, *J. Am. Chem. Soc.* **2004**, *126*, 6956–6966; c) D. Yang, Y.-H. Zhang, B. Li, D.-W. Zhang, *J. Org. Chem.* **2004**, *69*, 7577–7581.

[5] a) D. Yang, J. Qu, W. Li, Y.-H. Zhang, Y. Ren, D.-P. Wang, Y.-D. Wu, *J. Am. Chem. Soc.* **2002**, *124*, 12410–12411; b) D. Yang, X. Li, Y. Sha, Y.-D. Wu, *Chem. Eur. J.* **2005**, *11*, 3005–3009; c) X. Li, B. Shen, X.-Q. Yao, D. Yang, *J. Am. Chem. Soc.* **2007**, *129*, 7264–7265.

[6] D. Yang, D.-W. Zhang, Y. Hao, Y.-D. Wu, S.-W. Luo, N.-Y. Zhu, *Angew. Chem.* **2004**, *116*, 6887–6890; *Angew. Chem. Int. Ed.* **2004**, *43*, 6719–6722.

[7] a) D. H. Appella, L. A. Christianson, D. A. Klein, M. R. Richards, D. R. Powell, S. H. Gellman, *J. Am. Chem. Soc.* **1999**, *121*, 7574–7581; b) J. Applequist, K. A. Bode, D. H. Appella, L. A. Christianson, S. H. Gellman, *J. Am. Chem. Soc.* **1998**, *120*, 4891–4892; c) D. H. Appella, L. A. Christianson, D. A. Klein, D. R. Powell, X. Huang, J. J. Barchi, S. H. Gellman, *Nature* **1997**, *387*, 381–384.

[8] T. A. Martinek, G. K. Toth, E. Vass, M. Hollosi, F. Fulop, *Angew. Chem.* **2002**, *114*, 1794–1797; *Angew. Chem. Int. Ed.* **2002**, *41*, 1718–1721.

[9] D. Seebach, S. Abele, K. Gademann, G. Guichard, T. Hintermann, B. Jaun, J. L. Matthews, J. V. Schreiber, L. Oberer, U. Hommel, H. Widmer, *Helv. Chim. Acta* **1998**, *81*, 932–982.

[10] a) J. M. Langenhan, I. A. Guzei, S. H. Gellman, *Angew. Chem.* **2003**, *115*, 2504–2507; *Angew. Chem. Int. Ed.* **2003**, *42*, 2402–2405; b) Y. J. Chung, B. R. Huck, L. A. Christianson, H. E. Stanger, S. Krauthauser, D. R. Powell, S. H. Gellman, *J. Am. Chem. Soc.* **2000**, *122*, 3995–4004; c) D. Seebach, S. Abele, K. Gademann, B. Jaun, *Angew. Chem.* **1999**, *111*, 1700–1703; *Angew. Chem. Int. Ed.* **1999**, *38*, 1595–1597; d) X. Daura, K. Gademann, H. Schaefer, B. Jaun, D. Seebach, W. F. van Gunsteren, *J. Am. Chem. Soc.* **2001**, *123*, 2393–2404; e) Y. J. Chung, L. A. Christianson, H. E. Stanger, D. R. Powell, S. H. Gellman, *J. Am. Chem. Soc.* **1998**, *120*, 10555–10556; f) S. Krauthäuser, L. A. Christianson, D. R. Powell, S. H. Gellman, *J. Am. Chem. Soc.* **1997**, *119*, 11719–11720.

[11] a) S. Hanessian, X. Luo, R. Schaum, *Tetrahedron Lett.* **1999**, *40*, 4925–4929; b) M. Brenner, D. Seebach, *Helv. Chim. Acta* **2001**, *84*, 2155–2166; c) S. Hanessian, X. Luo, R. Schaum, S. Michnick, *J. Am. Chem. Soc.* **1998**, *120*, 8569–8570; d) D. Seebach, L. Schaeffer, M. Brenner, D. Hoyer, *Angew. Chem.* **2003**, *115*, 800–802; *Angew. Chem. Int. Ed.* **2003**, *42*, 776–778.

[12] T. S. Haque, J. C. Little, S. H. Gellman, *J. Am. Chem. Soc.* **1994**, *116*, 4105–4106.

[13] G. T. Copeland, E. R. Jarvo, S. J. Miller, *J. Org. Chem.* **1998**, *63*, 6784–6785.

[14] a) X. Wang, J. F. Espinosa, S. H. Gellman, *J. Am. Chem. Soc.* **2000**, *122*, 4821–4822; b) M. Rueping, J. V. Schreiber, G. Lelais, B. Jaun, D. Seebach, *Helv. Chim. Acta* **2002**, *85*, 2577–2593; c) D. Seebach, M. Brenner, M. Rueping, B. Jaun, *Chem. Eur. J.* **2002**, *8*, 573–584; d) H. S. M. Lu, M. Volk, Y. Kholodenko, E. Gooding, R. M. Hochstrasser, W. F. DeGrado, *J. Am. Chem. Soc.* **1997**, *119*, 7173–7180; e) J. S. Albert, M. W. Peczuh, A. D. Hamilton, *Bioorg. Med. Chem.* **1997**, *5*, 1455–1467; f) M. Yu, A. P. Nowak, T. J. Deming, D. J. Pochan, *J. Am. Chem. Soc.* **1999**, *121*, 12210–12211.

[15] Gaussian 98, Revision A.1, M. J. Frisch, G. W. Trucks, H. B. Schlegel, G. E. Scuseria, M. A. Robb, J. R. Cheeseman, V. G. Zakrzewski, J. A. Montgomery, Jr., R. E. Stratmann, J. C. Burant, S. Dapprich, J. M. Millam, A. D. Daniels, K. N. Kudin, M. C. Strain, O. Farkas, J. Tomasi, V. Barone, M. Cossi, R. Cammi, B. Mennucci, C. Pomelli, C. Adamo, S. Clifford, J. Ochterski, G. A. Petersson, P. Y. Ayala, Q. Cui, K. Morokuma, D. K. Malick, A. D. Rabuck, K. Raghavachari, J. B. Foresman, J. Cioslowski, J. V. Oritz, B. B. Stefanov, G. Liu, A. Liashenko, P. Piskorz, I. Komaromi, R. Gomperts, R. L. Martin, D. J. Fox, T. Keith, M. A. Al-Laham, C. Y. Peng, A. Nanayakkara, C. Gonzalez, M. Challacombe, P. M. W. Gill, B. G. Johnson, W. Chen, M. W. Wong, J. L. Andres, M. Head-Gordon, E. S. Replogle, J. A. Pople, Gaussian, Inc., Pittsburgh, PA, **1998**.

[16] a) A. D. Becke, *J. Chem. Phys.* **1993**, *98*, 5648–5652; b) B. Miehlich, A. Savin, H. Stoll, H. Preuss, *Chem. Phys. Lett.* **1989**, *157*, 200–206; c) C. Lee, W. Yang, G. Parr, *Phys. Rev. B* **1988**, *37*, 785–789.

[17] a) C. Moller, M. S. Plesset, *Phys. Rev.* **1934**, *46*, 618–622; b) N. C. Handy, H. F. Schaefer III, *J. Chem. Phys.* **1984**, *81*, 5031–5033; c) M. Head-Gordon, T. Head-Gordon, *Chem. Phys. Lett.* **1994**, *220*, 122–128.

[18] a) M. T. Cances, B. Mennucci, J. Tomasi, *J. Chem. Phys.* **1997**, *107*, 3032–3041; b) M. Cossi, V. Barone, B. Mennucci, J. Tomasi, *Chem. Phys. Lett.* **1998**, *286*, 253–260; c) B. Mennucci, J. Tomasi, *J. Chem. Phys.* **1997**, *106*, 5151–5158; d) M. Cossi, G. Scalmani, N. Rega, V. Barone, *J. Chem. Phys.* **2002**, *117*, 43–54.

[19] F. Chen, K. S. Song, Y. D. Wu, D. Yang, *J. Am. Chem. Soc.* **2008**, *130*, 743–775.

[20] The synthesis of compounds **1**–**7**; ^{1}H NMR spectroscopic data for the dilution and [D$_6$]DMSO addition experiments of **1**–**7**; 2D NOESY spectra of **1**–**7**; CD spectra of **2** and **4**–**7**; X-ray crystallographic structural analyses of **1** and **5**, including tables of bond lengths and angles; X-ray crystallographic data; tables of calculated energies and structures of model compounds **8**–**11**; and Cartesian coordinates of the structures are given in the Supporting Information.

Received: June 2, 2009
Revised: August 24, 2009
Published online: October 28, 2009

